Glycoconjugate Journal (1997) **14:** 935–943

EGC1
NMR analysis of carbohydrates with model-free spectral densities: the dispersion range revisited

L. Catoire[1], I. Braccini[1], N. Bouchemal-Chibani[1], L. Jullien[1], C. Herve du Penhoat[1]* and S. Perez[2]

[1] *Dpt de Chimie CNRS URA 1679, Ecole Normale Superieure, 24 rue Lhomond, 75231 Paris Cedex 05*
[2] *Ingenierie Moleculaire, INRA, BP527, 44316 Nantes*

Over the past decade molecular mechanics and molecular dynamics studies have demonstrated considerable flexibility for carbohydrates. In order to interpret the corresponding NMR parameters, which correspond to a time-averaged or 'virtual' conformer, it is necessary to simulate the experimental data using the averaged geometrical representation obtained with molecular modelling methods. This structural information can be transformed into theoretical NMR data using empirical Karplus-type equations for the scalar coupling constants and the appropriate formalism for the relaxation parameters. In the case of relaxation data, the 'model-free' spectral densities have been widely used in order to account for the internal motions in sugars. Several studies have been conducted with truncated model-free spectral densities based on the assumption that internal motion is very fast with respect to overall tumbling.

In this report we present experimental and theoretical evidence that suggests that this approach is not justified. Indeed, recent results show that even in the case of moderate-sized carbohydrates internal motions are occurring on the same timescale as molecular reorientation. Simulations of relaxation parameters (NOESY volumes, proton cross-relaxation rates, carbon T_1 and nOe values) in the dispersion range ($0.1 < \tau_c < 5$ ns) show that rates of internal motion can be fairly precisely defined with respect to overall tumbling. Experimental data for a variety of oligosaccharides clearly indicate similar timescales for internal and overall motion.

***Keywords*: model-free spectral densities, correlation time, relaxation**

Introduction

Over the past decade the goals in structural determinations of biomolecules have evolved dramatically. In keeping with the 'lock and key principle' [1], efforts were initially directed towards establishing a single conformation. However, due to advances in molecular modelling and NMR spectroscopy it became evident that, in the case of carbohydrates (and many other biomolecules) several families of low-energy conformers often coexist. As a result, conformational analysis with combined NMR and molecular modelling methods leads to an equilibrium ensemble or 'virtual structure'.

In parallel, several approaches have been developed for the detection of internal motion by NMR spectroscopy [2]. This area of research [3] has been stimulated by the conviction that conformational fluctuations are important for biological activity. In the case of disaccharides [4], this hypothesis was formulated 25 years ago and it was shown that a strong correlation exists between types of glycosidic linkages (classified according to their flexibility) and biological functions. In order to understand the role of internal motion, the question which must first be addressed is 'how to quantify this phenomenon'.

NMR relaxation data are a sensitive probe of fast intramolecular processes such as conformational fluctuations. However, interpretation of the experimental relaxation rates requires a physical motional model which is incorporated in the expressions for the spectral densities (equations 3 and 6, *vide infra*). The model-free approach is widely used in this connection as internal motion is defined by only two variables, the order parameter, S^2, which describes its spatial restriction or amplitude (S^2 is equal to 1 for totally restricted motion and to 0 for totally unrestricted motion) and τ_e, which is the corresponding effective correlation time (equation 7, *vide infra*). In the case of very rapid intramolecular processes where $\tau_e \ll \tau_c$ (τ_c, overall tumbling time), only S^2 is accessible from relaxation data whereas in

* To whom correspondence should be addressed.

0282–0080

the case of conformational fluctuations comparable in rate with molecular reorientation ($1 < \tau_e/\tau_c < 10$) both parameters are relaxation active [5].

Fairly different representations of internal motions of sugars have been reported based on NMR relaxation data [6] and/or MD studies [7]. In the present work, simulations of several types of experimental relaxation parameters with the model-free spectral densities have been evaluated in an attempt to obtain a unified description of the internal dynamics of carbohydrates.

Material and methods

Compounds **1** (galacturonic acid dimer), **2** (β-ethyllactoside), **3** (pentassacharide related to inulin) have been described in previous studies [2g] and the synthesis of (per-2,3-di-*O*-benzyl-per-6-*O*-(2-methoxy)-6-naphthoyl)-β-cyclodextrin **4** has been reported recently [8], Figure 1.

N.M.R. Spectroscopy

The spectral assignments of compounds **1**, **2**, and **3** have been reported and that of **4** will be given in a separate account. Proton relaxation data were acquired at 400.13 MHz as previously described [9]. NOESY spectra were acquired with mixing times of 0 and 1 (0.4 for **4**) s. The recycle time was set to $5 \times T_1$ in order to obtain a symmetrical normalized NOESY volume matrix. Diagonal and cross-peak intensities were evaluated from the summed ω_1 sub-spectra contributing to a specific signal. ^{13}C T_1 measurements were acquired using the inversion-recovery sequence (180-τ-90- FID). Heteronuclear nOes were measured with the inverse-gated technique. Finally, the DANTE-Z sequence [10] was used for the selective pulse in the measurements of selective proton longitudinal relaxation rates.

Simulations of relaxation data

The following expressions for the model-free spectral densities were used in order to obtain the plots in Figures 2–7. 100.6 MHz carbon relaxation parameters were simulated for methane carbons with a carbon-proton bond-length of 1.11 Å whereas the 400.13 MHz relaxation data have been simulated for two spins separated by 2.45 Å.

$$\frac{1}{T_1} = K\{J_0(\omega_H - \omega_C) + 3J_1(\omega_C) + 6J_2(\omega_H + \omega_C)\}$$

Equation 1

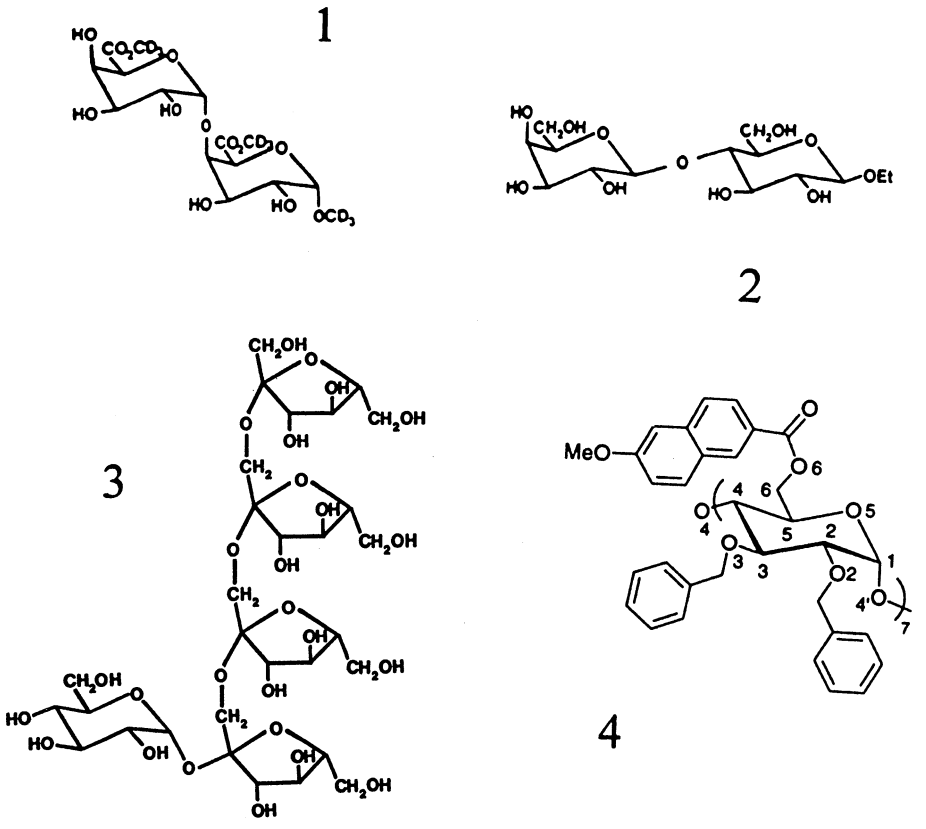

Figure 1. Schematic drawing of carbohydrates **1–4.**

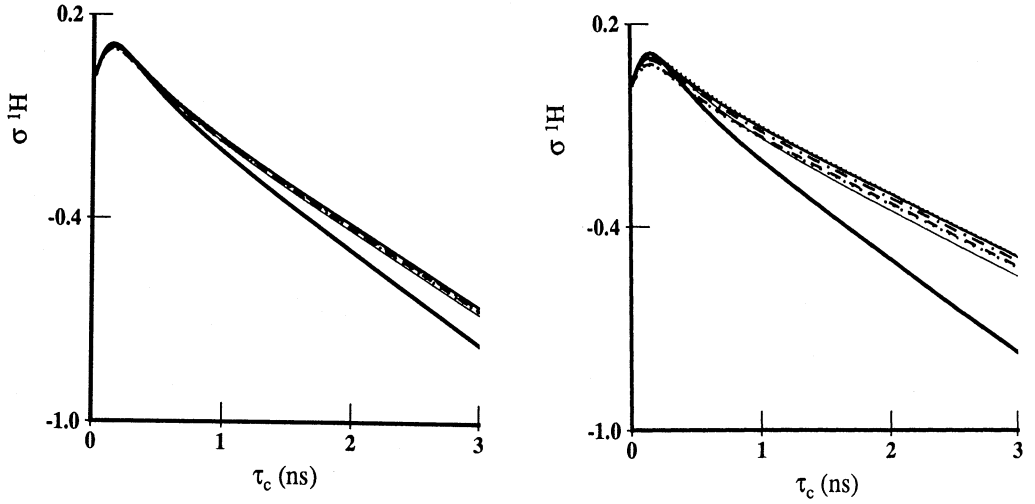

Figure 2. Plots of 400.13 MHz proton cross-relaxation rates, $\sigma_{k,l}$, as a function of τ_c established with the model-free spectral densities. The values of the angular order parameter, S^2_{ang} , were 0.9 (left) and 0.7 (right) and the values of τ_e were as follows: 1 (dotted), 10 (dashed), 50 (steeple), 100 (solid), 200 (thin dots) and 800 (thin solid) ps. The plot for a rigid molecule is given in bold.

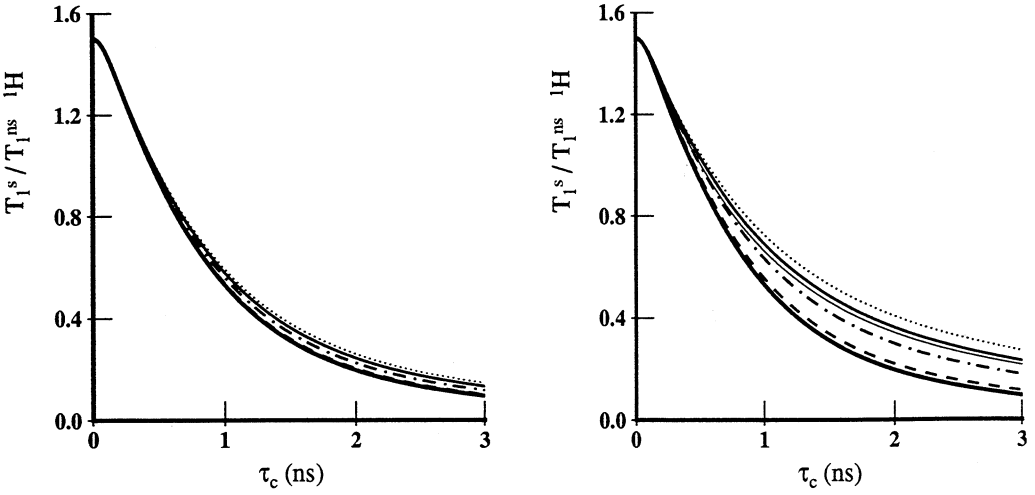

Figure 3. Plots of 400.13 MHz T_1^S/T_1^{NS} ratios as a function of τ_c established with the model-free spectra densities. The values of the dynamic parameters are the same as in Figure 2.

$$nOe = 1 + \eta = 1 + \frac{\gamma_H}{\gamma_C}\cdot\left\{\frac{6J_2(\omega_H+\omega_C) - J_0(\omega_H-\omega_C)}{J_0(\omega_H-\omega_C) + 3J_1(\omega_C) + 6J_2(\omega_H+\omega_C)}\right\} \quad \text{Equation 2}$$

$$J(\omega) = \frac{2}{5}\left\{\frac{S^2\cdot\tau_c}{1+(\omega\cdot\tau_c)^2} + \frac{(1-S^2)\cdot\tau}{1+(\omega\cdot\tau)^2}\right\} \quad \text{Equation 3}$$

$$\sigma_{k,l} = K'\{6J_2(2\omega) - J_0(0)\} \quad \text{Equation 4}$$

$$T_1^S/T_1^{nS} = \frac{6J_2(2\omega) + 3J_1(\omega) + J_0(0)}{12J_2(2\omega) + 3J_1(\omega)} \quad \text{Equation 5}$$

where the proton spectral density is as follows:

$$J_n(\omega) = \frac{2}{5}\left\{\frac{S^2\cdot\tau_c}{1+(\omega\cdot\tau_c)^2} + (\langle r^{-6}\rangle - S^2)\frac{\tau}{1+(\omega\cdot\tau)^2}\right\} \quad \text{Equation 6}$$

$$\text{with } \tau^{-1} = \tau_c^{-1} + \tau_e^{-1} \text{ and } S^2 = S^2_{ang}\cdot\left(\frac{1}{\langle r^3\rangle}\right)^2 \quad \text{Equation 7}$$

where $K = 0.1\ \gamma_H^2\gamma_c^2\hbar^2\, r_{C-H}^{-6}$ and $K' = 0.1\gamma_H^4\hbar^2$.

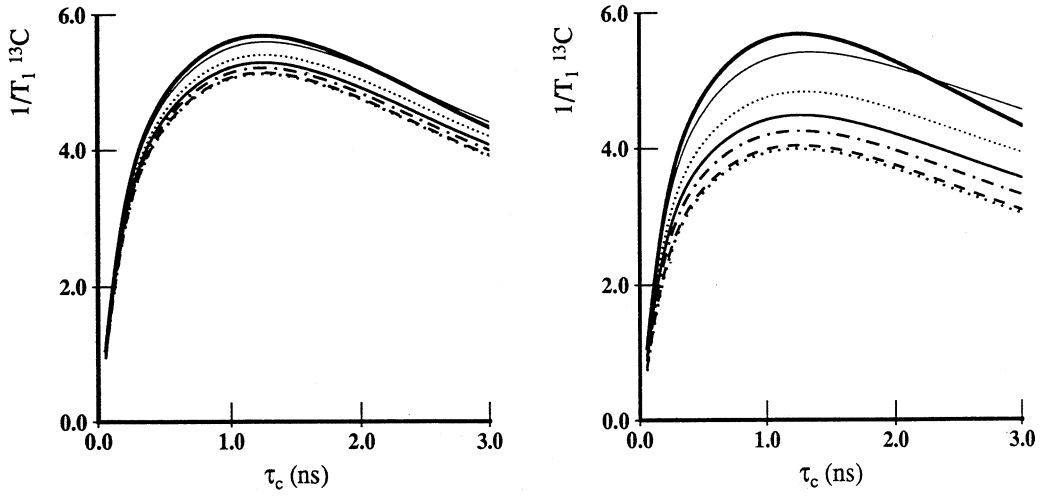

Figure 4. Plots of the 100.6 MHz carbon longitudinal relaxation times, T_1, as a function of τ_c established with the model-free spectral densities. The values of the dynamic parameters are the same as in Figure 2.

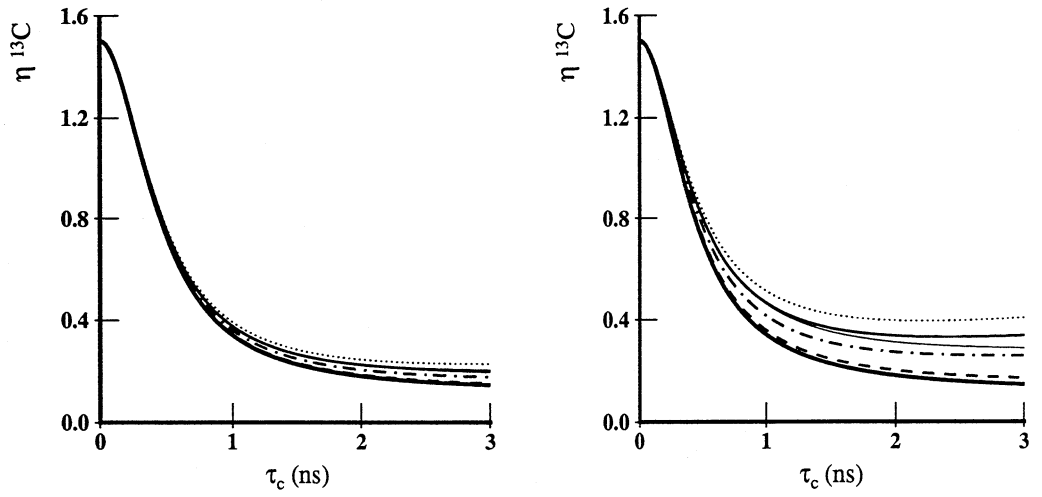

Figure 5. Plots of the 100.6 MHZ heteronuclear nOes as a function of τ_c established with the model-free spectral densities. The values of the dynamic parameters are the same as in Figure 2.

Results and discussion

A widely-used approach for establishing a physical motional model consists of least-squares fitting of the relaxation data of spins that are separated by a fixed internuclear distance with the appropriate spectral densities (*eg* C–H groups, methylene protons, ortho protons of an aromatic ring) [11]. These NMR data, which are independent of molecular geometry, mainly reflect molecular dynamics. On the basis of multi-field relaxation measurements, it is possible to evaluate τ_c, S^2, and eventually τ_e (when τ_e and τ_c are occurring on comparable timescales).

We have recently reported a related method [12] wherein theoretical NOESY volumes are least-squares fitted to all available experimental NOESY data (both diagonal and cross-peak volumes). In this protocol, structural groups are defined (methylene groups, cyclic protons of a common ring etc), which then share an average value of S^2_{ang} and τ_e. The physical models thus generated are considered to be viable if they are also able to reproduce the available carbon relaxation data.

When this approach was applied to a variety of disaccharides two distinct types of motional models emerged [12]. In the first model, **A**, order parameters were fairly

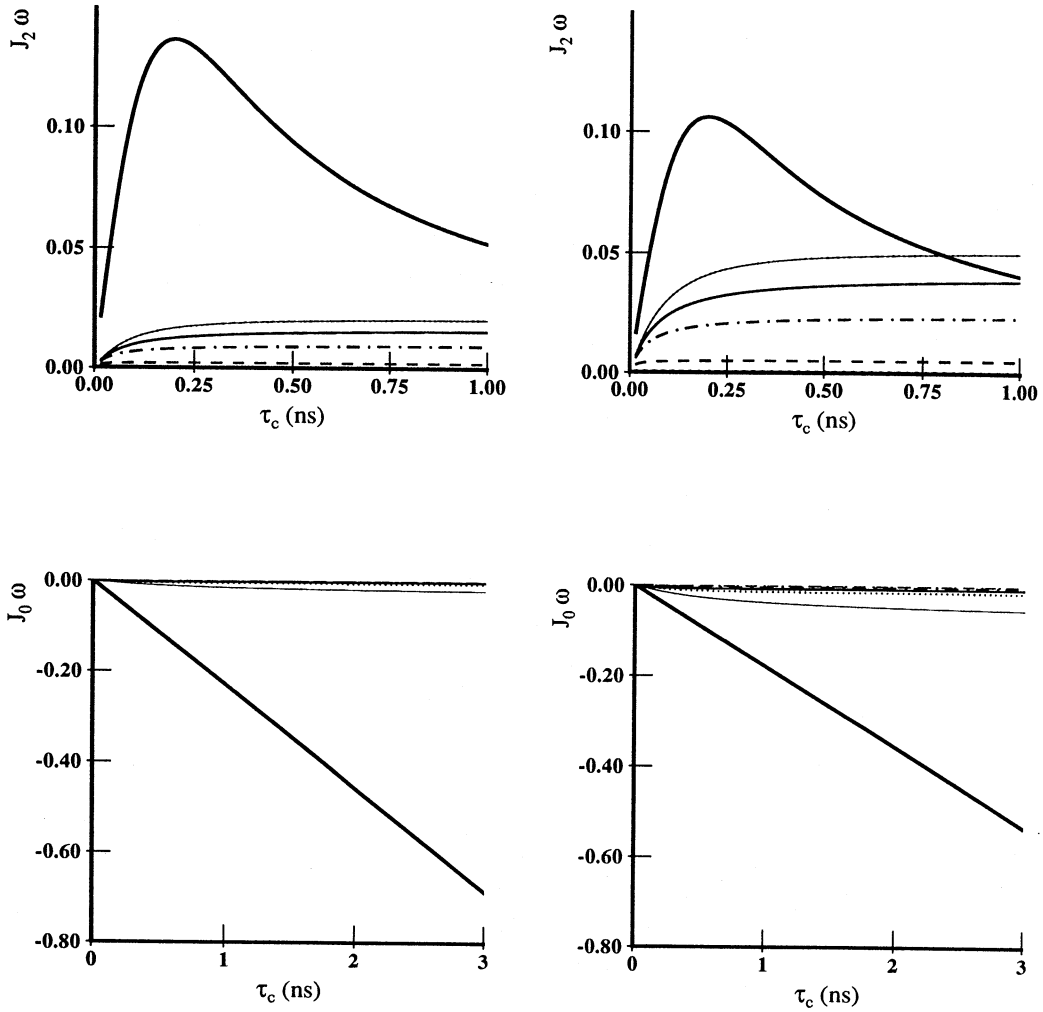

Figure 6. Plots of 400.13 MHz proton spectral densities, $6J_2(2\omega)$ (top) and $-1J_0(0)$ bottom), established with the model-free spectral densities. The contribution of the first term is given in bold and the values of the order parameter, S^2, were 0.9 (left) and 0.7 (right). The second term is indicated with the same key as in Figure 2.

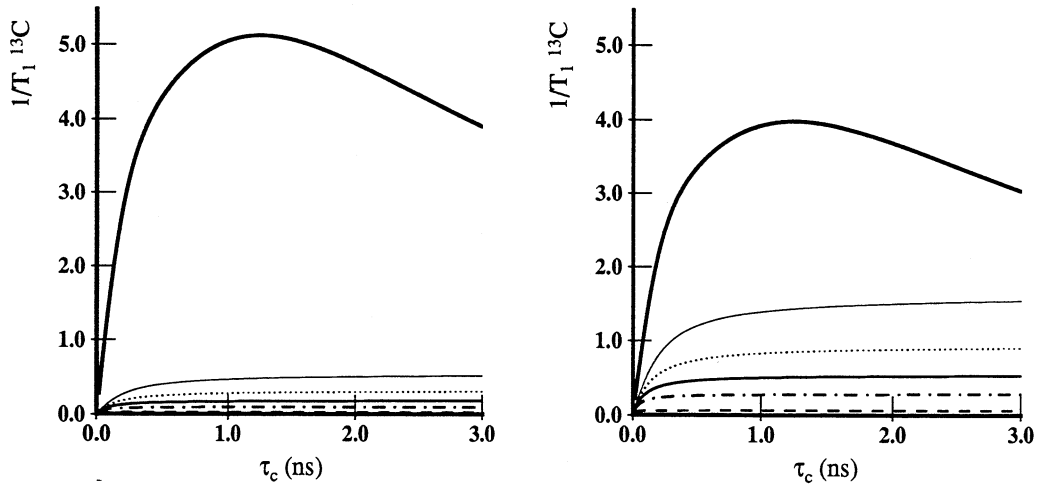

Figure 7. Plots of 100.6 MHz carbon longitudinal relaxation times, T_1, established with the model-free spectral densities. The contribution of the first term is given in bold and the values of the angular order parameter, S^2_{ang}, were 0.9 (left) and 0.7 (right). The second term is indicated with the same key as in Figure 2.

high, > 0.9 and the effective correlation time for the internal motion was very fast (< 10 ps). In the second model, **B**, order parameters were much lower and the internal motion occurred on a timescale comparable to that of overall motion (50–200 ps). Truncated model-free spectral densities (only the first term in equations 3 and 6) would be appropriate for **A** which corresponds to a fairly rigid molecule whereas the complete expression would be required for more flexible structures such as those associated with model **B**.

In order to visualize the effect of internal motion on laboratory-frame NMR relaxation parameters, data have been simulated for two protons separated by 2.45 Å [*ie* typical vicinal axial/equatorial protons of sugars] (Figures 2 and 3) and a methane carbon with C–H bond and length of 1.11 Å (Figures 4 and 5). In the following discussion S^2 will be used to designate order parameters but in the case of homonuclear relaxation data, it is tacitly understood that S^2 is to be replaced by S^2_{ang}. Parameters have been plotted as a function of τ_c for an almost rigid model ($S^2 = 0.9$, plots on the left) and for a more flexible one ($S^2 = 0.7$, plots on the right). Six τ_e values between 1 and 800 picoseconds have been considered (see the key) and for comparative purposes, the rigid molecule parameters are given as a function of τ_c in bold on all plots.

Two types of relaxation parameters have been considered, ones which are a linear function of spectral densities, P1 (proton cross-relaxation rates, Figure 2, and carbon longitudinal relaxation rates, Figure 4), and ones which are a function of the ratios of spectral densities, P2 (proton T_1^S/T_1^{NS} ratios where S stands for selective and NS stands for non-selective, Figure 3, and carbon nOe factors, Figure 5). From Figures 2 and 4, it can be seen that the first category of relaxation parameters is very sensitive to the S^2 value and as the amplitude of motion increases (*ie* when S^2 decreases) the influence of the rate of internal motion becomes important (contribution of the second term of the spectral densities). In contrast, the second category of relaxation parameters, Figures 3 and 5, is fairly insensitive to the S^2 value for very fast internal motion ($\tau_e < 50$ ps). However, in the case of less restricted motion ($S^2 = 0.7$) which is occurring at a comparable rate to that of overall tumbling, a large influence on simulated data is observed (plots on the right).

Finally, the comparison of τ_c values extracted from these two types of relaxation data gives an indication of the amplitude of internal motion. For model **A**, relaxation parameters (P1) which are a linear function of spectral densities will be approximately equal to the product, $S^2 \cdot$(P1-rigid) whereas relaxation parameters (P2) which are a function of the ratio of spectral densities will be equal to (P2-rigid) as, in this case, in the corresponding expressions (equations 2 or 5) S^2 cancels out. The situation is less straight-forward for model **B** but a large discrepancy in the τ_c values extracted from the two types of relaxation data strongly suggest the presence of internal dynamics. Such comparisons have been recommended for the detection of internal motion [2a,g].

Carbon T_1 values for compound **1** have been collected in Table 1. These data are very homogeneous indicating isotropic overall reorientation and either the absence of internal motion or uniform internal dynamics. The τ_c value for a rigid molecule ($S^2 = 1$) is 0.12 ns and, as can be seen in Figure 4, this value must be increased (0.15–0.18 ns) for a model with moderate amplitude ($S^2 = 0.8$) of internal motion. Comparison of the experimental NOESY data (**bold**), Table 2 with those calculated for either a rigid (*italics*) or a moderately-flexible (third value; $S^2 = 0.8$, $\tau_e = 0.14$ ns) model indicates reasonable agreement with the fit being slightly better for the latter model (see encased values). It is to be noted that relaxation due to sources other than intramolecular dipole-dipole has been ignored and, therefore, the theoretical volumes should be slightly larger than the experimental ones. Inspection of the theoretical plots for the carbon T_1s and proton cross-relaxation rates shows, that upon simultaneously increasing S^2 and decreasing τ_c, one would undoubtedly obtain a continuum of models between **A** and **B** capable of reproducing a given P1 data set.

The contributions of the first (bold) and second (see key) terms of the model-free spectral densities to proton cross-relaxation rates, Figure 6, and to carbon longitudinal relaxation rates, Figure 7, have been plotted separately as a function of τ_c for S^2 values of 0.9 (left) and 0.7 (right). In the case of disaccharides, τ_c values are in the 0.1–0.2 ns range. For the carbon data, in going from model **B** to model **A** (where S^2 increases and τ_c decreases), a decrease in the contribution of the second term of the model-free spectral densities is compensated by an increase in the first term. For proton cross-relaxation rates of disaccharides the situation is more complicated. Here, a decrease in the second term of $6 \cdot \boldsymbol{J}(2\omega)$ is offset by an increase in the first term of $-1 \cdot \boldsymbol{J}(0)$ (which becomes less negative) and an increase in the first term of $6 \cdot \boldsymbol{J}(2\omega)$. It is noteworthy that for an S^2 value of 0.7, the contribution of the second term in Figure 6 is larger than that of the first term for τ_c values larger than 0.8 ns. These values of the tumbling time still correspond to fairly

Table 1. 100.6 MHz Carbon longitudinal relaxation times of **1**.

Carbon	*C1′*	*C2′*	*C3′*	*C4′*	*C5′*	*C1*	*C2*	*C3*	*C4*	*C5*
T1(s)	0.40	0.39	0.43	0.43	0.41	0.44	0.40	0.45	0.41	0.43

Table 2. Theoretical[a] and experimental normalized NOESY volumes (**in bold**) for compound **1** in D_2O at 296 K (400.13 MHz – internal ref.: DMSO).

^{1}H	1′	2′	3′	4′	5′	1	2	3	4	5
	0.416	**−0.061**	**−0.007**		**−0.002**				**−0.056**	
1′	*0.398*	*−0.051*	*−0.002*		*−0.003*				*−0.055*	
	0.440	−0.062	−0.002		−0.003				−0.059	
		0.580	**−0.008**	**−0.006**	**−0.007**		**−0.008**	**−0.008**		**−0.004**
2′		0.548	−0.013	*−0.003*	*−0.002*		*−0.002*	*−0.002*		*0*
		0.641	−0.015	−0.003	−0.002		−0.002	−0.002		0
3′			**0.470**	**−0.045**	**−0.039**		**−0.011**			
			0.470	*−0.047*	*−0.032*		*−0.005*			
			0.536	−0.053	−0.036		−0.006			
4′				**0.450**	**−0.034**		**−0.005**			
				0.488	*−0.044*		*−0.001*			
				0.561	−0.049		−0.001			
					0.460		**−0.019**			
5′					*0.452*		*−0.019*			
					0.512		−0.021			
1						**0.601**	**−0.056**	**−0.010**		**−0.002**
						0.593	*−0.058*	*−0.003*		*−0.005*
						0.696	−0.006	−0.003		−0.006
2							**0.510**	**−0.003**	**−0.007**	**−0.007**
							0.495	*−0.012*	*−0.002*	*−0.002*
							0.564	−0.012	−0.002	−0.002
3								**0.450**	**−0.035**	**−0.047**
								0.458	*−0.038*	*−0.043*
								0.512	−0.041	−0.048
4									**0.290**	**−0.041**
									0.336	*−0.035*
									0.356	−0.038
										0.480
5										*0.488*
										0.552

[a] Theoretical volumes simulated for the rigid model $\tau_c = 1.2\,10{-}10$ s (*in Italics*), and for flexible model $\tau_c = 1.8\,10^{-10}$ s; $\tau_e = 1.44\,10^{-10}$ s and $S^2_{ang} = 0.85{-}0.89$ (normal).

small biomolecules but, of course, $J(0)$ already dominates proton relaxation.

In the case of compound **1**, two arguments in favour of the **B** model can be advanced. On the one hand, calculations of S^2 from *in vacuo* molecular dynamics trajectories lead to values in the 0.75–0.8 range [12]. On the other hand, a previous study of the internal dynamics of **1** based on comparison of τ_c values simulated for both carbon T_1s and the proton T_1^S/T_1^{NS} ratios (0.24 ns as compared to 0.33 ns at 10 °C) strongly suggested that the **B** model was the more appropriate one [2g].

A similar observation regarding the NMR relaxation data of sucrose (compound **2**) has been made recently [12]. All the experimental data can be reproduced with either **A** or **B** (associated with τ_e values in the 50–100 ps range) type models as described above. In this work, order parameters were calculated from a nanosecond condensed-phase molecular dynamics trajectory and these theoretical data were in excellent agreement with a flexible B-type model. Again, comparison of τ_c values simulated for both carbon T_1^S and the proton T_1^S/T_1^{NS} ratios (0.28 ns as compared to 0.29–0.58 ns at 4 °C) also pointed to a **B**-type model [2g].

Carbon relaxation data (T_1s and nOe factors) for the pentasaccharide, **3**, have been collected in Table 3 (from top to bottom of Figure 1, the fructofuranose residues of **3** are referred to as f‴, f″, f′ and f). From Figures 4 and 5 it can be seen, that for a given overall tumbling time, nOe factors increase when the rate of motion approaches τ_c. Under these conditions $1/T_1$ decreases. If one places the centre of gravity of **3** in the middle of the chain, then the relaxation

Table 3 100.6 MHz Carbon relaxation data[a] for compound **3**.

Parameter	*α-Glc*p			*β-Fruc*f		
	C1–C5[b]	*C6*		*C1*	*C3–C5*[b]	*C6*
			f	1.12	0.92 (0.00)[d]	
η	1.26 (0.03)	1.42	f″[c]	1.11	0.96 (0.03)[e]	1.13[f]
			f′ + f‴		1.04 (0.04)[e]	
			f	0.26	0.24 (0.00)[d]	0.34
NT1	0.29 (0.01)	0.34[c]	f″[c]	0.27	0.23 (0.01)[e]	0.36[g]
			f′ + f‴	0.28, 0.35	0.27 (0.02)[e]	

[a] Averaged values for two experiments.
[b] Averaged values for carbons C1 (C3 for β-Frucf) to C5; standard deviation in brackets.
[c] f′ and f″ can be reversed.
[d] Average deviation < 0.005.
[e] Averaged values for C3 and C4.
[f] Averaged value for all C6.
[g] Averaged value for f′, f″, f‴.

Table 4. 100.6 MHz Relaxation data[a,b] for anomeric carbons of compound **4**.

Parameter	*C1(1)*	*C1(2)*	*C1(3)*	*C1(4)*	*C1(5)*	*C1(6)*	*C1(7)*	*Average SD*
η	0.45	0.50	0.53	0.53	0.53	0.63	0.47	0.07
T1	0.18	0.17	0.17	0.17	0.15	0.17	0.15	0.07

[a] T1 values are the average of two experiments.
[b] η values are the average of four experiments.

data can be explained by considering that internal motion will increase from the centre of gravity outwards. The experimental values of the nOe factor are effectively higher for the Glc*p* (1.26) and f‴ Fru*f* rings (1.04) with respect to the f (0.92) and f″ (0.96) ones. Similarly, the carbon T_1s are lowest for the internal rings (0.23 and 0.24 s) with respect to the outer residues (0.29 and 0.27 s). The spread in nOe factors strongly suggests that internal motion is occurring on a similar time-scale to that of molecular reorientation. However, overall tumbling is tacitly assumed to be isotropic in the above reasoning and anisotropic overall motion would be expected to lead to variations in the carbon T_1 and nOe values. Insufficient data have been collected to determine the nature of overall tumbling and the only argument which supports isotropic tumbling is the fact that the experimental relaxation data are very homogeneous within a given ring.

The modified β-cyclodextrin, **4**, has a very spherical shape, Figure 8a,b, and here overall tumbling can be safely assumed to be isotropic. This carbohydrate exhibits two stable conformations at room temperature, both a symmetrical form (C_7) with seven equivalent sugar residues and an asymmetrical form (C_1) with seven distinct glucose rings. An appreciable exchange rate is not observed at temperatures below 100 °C. The conformational analysis of this molecule will be reported elsewhere and, in the following discussion, only data for the unsymmetrical conformer are given. The corresponding carbon relaxation data for the anomeric carbons (T_1s and nOe factors) have been collected in Table 4. The average T_1 value for all the anomeric carbons (0.16 s, 7 data points) is only slightly lower the average T_1 value for the totality of methine sugar carbons (0.18 s, 35 data points) and the latter value was used to establish a physical model. The corresponding $1/T_1$ value is compatible with a fairly wide spread of τ_c values (0.9 to 1.6 ns) due to the shape of the plot in Figure 4.

The large variation in nOe factors (0.45–0.63) clearly implies that the correlation time for internal motion is comparable to that of tumbling. It is interesting to note that the longest τ_c value that is compatible with the average nOe factor value is roughly 0.7 ns and thus no physical motional model based on very fast internal motion will be compatible for both sets of carbon data. Indeed, in the case of very rapid internal motion the nOe factor is insensitive to variations in S^2. Moreover, in order to account for the spread in nOe factors not only must τ_e be analogous to τ_c but also the amplitude of internal dynamics must vary considerably. Preliminary simulations of NOESY volumes (data not

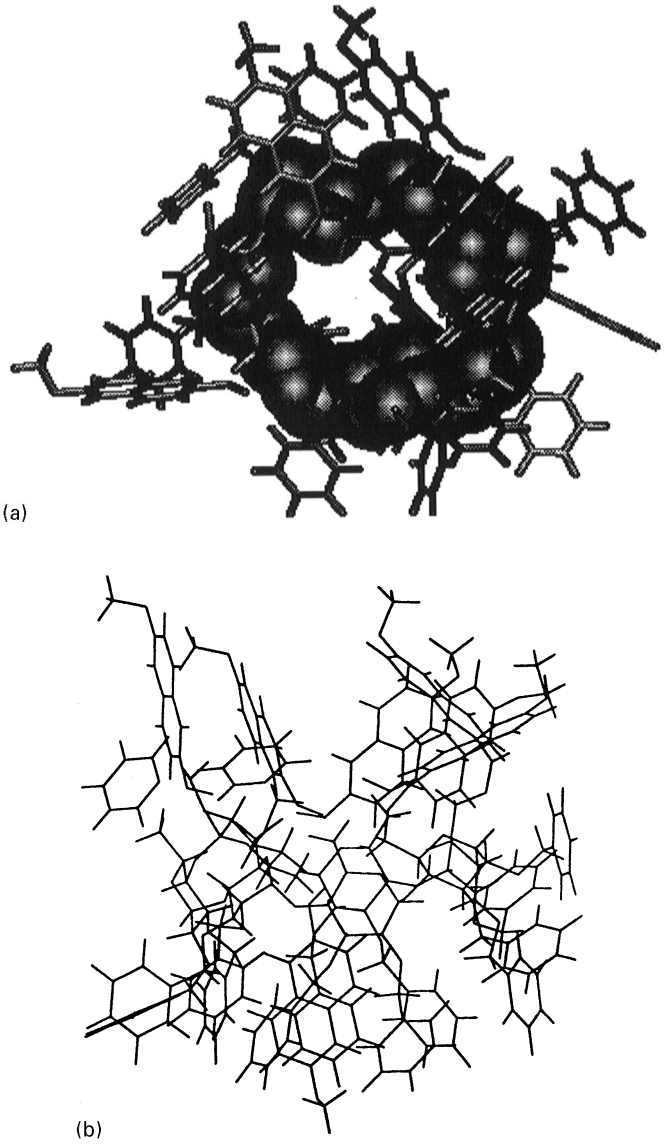

Figure 8. Optimized conformer of **4** viewed from above (left, the glucosyl atoms are presented as space-filled models) and from the side.

given) of **4** have narrowed the range of acceptable τ_c values considerably (0.8–1.0 ns).

Conclusions

Physical motional models have been established for compounds **1–4** from carbon relaxation data. In the case of disaccharides, two distincts types of models have emerged: an almost rigid model for which internal motion was considered to be extremely fast (picosecond timescale) and a more flexible one for which internal motion was considered to be slower (0.1–0.8 ns timescale). For larger molecules only the latter model can explain the experimental data.

In parallel, molecular dynamics calculations of order parameters of sugar [2f, 12] and the carbohydrate moieties in nucleic acids [14] have suggested that the second model is the more appropriate one. Moreover, several groups have reported correlation times for the internal motion of carbohydrates exocyclic groups [15, 16] and desoxyribose residues in nucleic acids [17] based on NMR relaxation data which also corroborate the second model. Finally, the simulations of relaxation data in the present work, which are representative of small-to-medium sized molecules, have shown that, for τ_c values of less than 3 ns, the second term of the model-free spectral densities can only be neglected for very restricted internal motion.

References

1 Kessler H (1982) *Angew Chem Int Ed Engl.* **21**: 518–23.
2 (a) McCain DC, Markley JL (1986) *J Am Chem Soc* **108**: 4259–64. (b) Mirau PA, Bovey FA (1986) *J Am Chem Soc* **108**: 5130–34. (c) Davis DG (1987) *J Am Chem Soc* **109**: 3471–72. (d) Simorre JP, Genest D (1990) *Magn Reson Chem* **28**: 21–4. (e) Goldman M, Desvaux H (1992) *C R Acad Sci Ser II* **317**: 749–56. (f) Hricovini M, Carver JP (1992) *Biochemistry* **31**: 10018–23. (g) Braccini I, Michon V, Herve du Penhoat C, Imberty A, Perez S (1993) *Int J Biol Macromol* **15**: 51–5.
3 Lane A (1993) *Prog NMR Spectroscopy*, **25**: 481–505.
4 Rees DA, Scott WE (1971) *J Chem Soc* ***B*** 469–79.
5 Bruschweiler R, Ernst RR (1992) *J Chem Phys* **96**: 1758–66.
6 Kowalewski J, Widmalm G (1994) *J Phys Chem* **98**: 28–34.
7 Engelsen SB, Perez S, Braccini I, Herve du Penhoat C (1995) *J Comput Chem* **16**: 1096–119.
8 Jullien L, Canceill J, Lacombe L, Lehn JM (1994) *J Chem Soc Perkin Trans* **2**: 989–1002.
9 Meyer C, Perez S, Herve du Penhoat C, Michon V (1993) *J Am Chem Soc* **115**: 10300–10.
10 Boudot D, Canet D, Brondeau J, Boubo JC (1989) *J Magn Reson* **83**: 428–39.
11 Craik DJ, Kumar A, Levy GC (1983) *J Chem Inf Comput Sci* **23**: 30–8.
12 Bouchemal-Chibani N, Braccini I, Derouet C, Herve du Penhoat C, Michon V (1995) *Int J Biol Macromol* **17**: 177–82.
13 Engelsen SB, Herve du Penhoat C, Perez S (1995) *J Phys Chem* **99**: 13334–51.
14 Koning TMG, Boelens R, van der Marel GA, van Boom JH, Kaptein R (1991) *Biochemistry* **30**: 3787–97.
15 Ejchart A, Dabrowsky J (1992) *Magn Reson Chem* **30**: 5115–5124.
16 Kovacs H, Bagley S, Kowalewski J (1989) *J Magn Reson* **85**: 530–41.
17 Boher PN, Laplante SR, Kumar A, Zanatta N, Martin A, Hakkinen A, Levy GC (1994) *Biochemistry* **33**: 2441–50.

Received 19 March 1996, accepted 4 June 1996